Copy
RM E57G16

NACA RM E57G16

NACA

RESEARCH MEMORANDUM

INVESTIGATION OF A CONTINUOUS NORMAL-SHOCK POSITIONING CONTROL FOR A TRANSLATING-SPIKE SUPERSONIC INLET IN COMBINATION WITH J34 TURBOJET ENGINE

By Fred A. Wilcox

Lewis Flight Propulsion Laboratory
Cleveland, Ohio

NATIONAL ADVISORY COMMITTEE
FOR AERONAUTICS

WASHINGTON

October 2, 1957

[redacted]

NATIONAL ADVISORY COMMITTEE FOR AERONAUTICS

RESEARCH MEMORANDUM

INVESTIGATION OF A CONTINUOUS NORMAL-SHOCK POSITIONING CONTROL FOR A TRANSLATING-SPIKE SUPERSONIC INLET IN COMBINATION WITH J34 TURBOJET ENGINE

By Fred A. Wilcox

SUMMARY

Use of a normal-shock positioning control was demonstrated at Mach numbers of 1.8 and 2.0 for a translating-spike supersonic inlet in combination with a J34 turbojet engine. Stable operation of the control was obtained which can be partly attributed to a nonlinearity in the servo valve in the null region.

INTRODUCTION

It is shown in reference 1 that matching of a supersonic inlet to an engine can be obtained by manipulating a bypass or a translating spike to control the position of the normal shock. In that report, data are presented for a simple on-off type control system. A faster responding continuous control system is desirable to maintain the inlet operating point near the optimum in the presence of disturbances caused either externally or by changes in engine airflow. Bypass controls of this type are presented in references 2 and 3. In order to design these faster responding controls, however, a knowledge of inlet dynamics is required. Some inlet dynamic data for the diffuser equipped with a bypass are presented in reference 4.

For the present investigation the translating spike of the inlet configuration used in reference 1 was fitted with a fast-acting hydraulic servo actuator. This permitted the use of a continuous spike control and also permitted obtaining inlet dynamic data by imposing sinusoidal oscillation to the spike.

This report presents some observations on the behavior of a continuous spike control using inlet normal-shock position as the controlled

[redacted]

variable. Also presented are some preliminary results of the inlet dynamics obtained with sinusoidal oscillations in spike and bypass positions.

SYMBOLS

A_f compressor frontal area, 1.978 sq ft

M Mach number

m mass flow, slugs/sec

P total pressure, lb/sq ft abs

w weight flow, lb/sec

$\frac{w\sqrt{\theta}}{A_f\delta}$ engine airflow corrected to standard conditions, based on compressor frontal area of 1.978 sq ft

δ ratio of total pressure to NACA standard sea-level pressure of 2116 lb/sq ft

θ ratio of total temperature to NACA standard sea-level temperature of 518.7° R

θ_l spike position angle, angle between inlet centerline and line joining spike tip and cowl lip, deg

Subscripts:

0 free stream

3 diffuser exit

APPARATUS AND PROCEDURE

The J34-engine - supersonic inlet configuration used in the 8- by 6-foot supersonic tunnel is described in references 1 to 5 and is shown schematically in figure 1. The critical inlet airflow could be matched to that required by the engine by either of two independent systems, a bypass or a translating spike. Both of these devices were operated by hydraulic servo actuators and were capable of spilling about 20 percent of the inlet mass flow.

4520

The position of the inlet normal shock was sensed by a flush static orifice located 2.9 inches downstream of the cowl lip. The orifice was connected to a miniature strain-gage-type pressure transducer by about 3 inches of tubing. Amplifier output was compared to a manually set reference voltage, and the resulting error signal fed into a servo amplifier. A switch permitted operation of either the spike or bypass servo systems.

An electronic function generator was used to supply the servo amplifier with a triangular wave shape at a frequency of 0.1 cycle per second for obtaining traces of the control signal pressure as the bypass and spike positions were varied. The function generator was also used to supply a sinusoidal wave form at frequencies up to 22 cycles per second for investigation of inlet dynamics. For this the amplitude of oscillation of the bypass and spike was held constant while the frequency was varied. The spike and bypass were oscillated about mean positions which located the inlet normal shock at the shock position sensing orifice. Spike and bypass positions and static orifice pressures were recorded on an optical-type oscillograph with galvanometer elements having natural frequencies of 200 cycles per second.

The hydraulic system was operated at a pressure of 1900 pounds per square inch. The rates of travel of both servo actuators against imposed error voltage are given in figure 2. A nonlinearity was obtained for both in the region of the null. A null shift of about 0.1 volt existed between the two servomechanisms. Although not shown in the figure, saturation was obtained at approximately ±0.7 volt for both.

The resulting control system for both the bypass and the spike was integral in behavior. The integrator rate consisted of the product of signal pressure gain, pressure transducer gain, and servomechanism gain. Integrator rates used were varied from 20 to 103 by changing the pressure transducer amplifier gain. Values of gain used in the control loop are listed in the following table:

System	Spike control	Bypass control
Signal pressure, (lb/sq ft)/in.	2160	1758
Servomechanism, (in./sec)/volt	35	35
Pressure transducer, volt/(lb/sq ft)	0.000245 to 0.00136	0.000338 to 0.001481

RESULTS AND DISCUSSION

The principle of inlet-engine matching using a translating spike is illustrated in figure 3. The lines shown are the envelope of critical operating points obtained from an investigation of the inlet for the bypass closed (ref. 5). The spike position angle θ_l required to give various percentages of rated corrected engine airflow is presented along with the resulting inlet mass-flow ratio and inlet total-pressure recovery. Operating points set by the control are included.

The inlet was sized for the engine airflow resulting at rated engine speed for the tunnel temperature conditions at a free-stream Mach number of 2.0. Inlet operation at a mass-flow ratio of 1.0 and near maximum inlet pressure recovery is obtained for these conditions. If the engine corrected airflow is decreased by reducing engine speed or by operating at a higher air temperature, critical operation could be maintained by extending the spike, which provides oblique-shock spillage. If the engine corrected airflow is increased by increasing engine speed or by operating at lower temperature, critical operation could be maintained by retracting the spike. This action would increase the corrected airflow by reducing the inlet pressure recovery (δ term in denominator of corrected airflow parameter $w\sqrt{\theta}/A_f\delta$) while not affecting the actual mass flow. Inlet pressure recovery is reduced at critical operation by having the oblique shock enter the cowl. The data points shown represent a variety of engine speed and bypass positions. Bypass and engine airflow were added to obtain the total which, in this case, was nearly constant. All the points shown resulted in inlet operation near the design point.

As the free-stream Mach number was lowered to 1.8 (fig. 3(b)), the inlet became oversized for the engine. This results from the airflow characteristics of the engine and the operating temperature of the tunnel. In order to operate the engine at rated engine speed (92.5 percent of rated corrected airflow), the spike would have to be positioned at a spike position angle θ_l of 43°, which would result in an oblique-shock spillage of about 7 percent. During control operation the engine was operated near rated engine speed while the bypass position was varied from closed to about half open, which accounted for airflows higher than the rated value. Data points set by the control illustrate that operation was maintained slightly supercritical.

Control signal pressures are presented in figure 4 where the normal shock was oscillated across the sensing orifice at a frequency of 0.1 cycle per second. The trace where the shock was oscillated by means of the bypass (fig. 4(a)) shows a considerable difference in the signal pressure for opening and closing the bypass. This is presumably caused by shock - boundary-layer interaction phenomena. The slope of the signal pressure curve used in determining system integrator rates is indicated by the dashed line.

The control signal pressures obtained with spike movement in either direction (fig. 4(b)) were more irregular than for the bypass and had several sharp discontinuities. It is felt that this greater irregularity can be partly attributed to a variation in flow area at the sensing station as the spike is translated. Because of the irregular nature of the signal pressure curves and the variation of spike travel with direction, the effective signal pressure gain is difficult to determine. Therefore, system integrator rates were determined by assuming the signal pressure gain (dashed line). As will be shown later, the effective slope for the spike control appears to be greater than indicated by the dashed line. Mean values of the control signal pressures in terms of spike position angle are presented in figure 5 for free-stream Mach numbers of 1.8 and 2.0.

The change in air mass spillage provided by a given change in bypass door position was the same (constant gain) regardless of the initial position of the door because the discharge area was nearly a linear function of position. The effectiveness of the spike in controlling mass spillage, however, varied greatly with its position (see fig. 6). At Mach number 2.0, for example, 1 inch of spike travel can result in a change of from 6.6 to 9.3 percent of corrected airflow at critical operation depending on the spike position. At Mach number 1.8 this can vary from 2.5 to 10 percent. This variation in effectiveness results from the combined effects of actual mass spillage and changes in diffuser pressure recovery. More effectiveness is obtained at the lower values of θ_l where the oblique shock falls ahead of the cowl.

Response time is presented in figure 7 for both controls. For these data the engine speed was set so that either the bypass or spike was positioned at about the midpoint by the control being tested. Then the control was disturbed by manually extending or retracting either actuator the full amount, which resulted in an approximate 10-percent disturbance of engine airflow. Response time presented is the time required to restore the bypass or spike to within 10 percent of its original position. Response time decreased with increasing integrator rate in approximately the same manner for both controls. There was a tendency for the spike to have lower response time for supercritical displacement than for subcritical displacement. This results from higher rates of change of inlet airflow for low θ_l as shown on figure 6. Control overshoot is presented in figure 7 in terms of control signal overshoot in pounds per square foot with lines drawn through the maximum values obtained. The bypass control had generally lower response time and more overshoot than the spike.

Stable operation of both controls was obtained for all integrator rates used. A contributing factor to this stability is believed to be the nonlinearity in the servo valves in the null region as shown in figure 2. This reduction in servomechanism gain in the null region has a stabilizing influence by reducing loop gain at the control operating point while giving high loop gain for operation away from the control point. Other examples of servo-valve nonlinearity and null shift are discussed in reference 6.

Typical traces from which the response data were obtained are presented in figure 8. For these traces the bypass was closed manually and the spike was retracted manually, which put the inlet into a subcritical operating condition. Because of the initial slightly supercritical operating point set by the control, inlet buzz was not obtained in either case. The greater overshoot and faster response of the bypass control suggest that the effective slope of the control signal pressure (fig. 4(a)) was steeper than that used in determining the integrator rates. 4520

A comparison of phase shift of the shock position sensing pressure in response to sinusoidal oscillations of the bypass and spike is given in figure 9. These data are preliminary results of data taken for a range of inlet conditions at Mach numbers of 1.8 and 2.0. Somewhat more phase shift is noted for the bypass than was obtained at Mach number 2.0 in a previous investigation (ref. 4). The amount of phase shift obtained with the spike was considerably less than that obtained with the bypass (approximately half as much for the data shown). The phase shift for bypass oscillation is believed to result from a dead time (wave propagation time from the bypass to the cowl lip) plus a lag (fill up time). The phase shift obtained with the spike is presumably less because of shorter dead time.

CONCLUDING REMARKS

In an investigation of a continuous normal-shock spike control on the inlet of a J34-engine installation in the 8- by 6-foot supersonic tunnel, stable operation was obtained for all integrator rates used in spite of a control pressure signal which varied with the direction of the shock movement. A nonlinearity in the servo valve in the null region is believed to be a contributing factor to this stability. The spike control had a tendency for faster response when operating with the spike in the extended position because of greater effectiveness of the spike in spilling air in this position.

Lewis Flight Propulsion Laboratory
National Advisory Committee for Aeronautics
Cleveland, Ohio, July 18, 1957

REFERENCES

1. Leissler, L. Abbott, and Nettles, J. Cary: Investigation to Mach Number 2.0 of Shock-Positioning Control Systems for Variable-Geometry Inlet in Combination with a J34 Turbojet Engine. NACA RM E54I27, 1954.

2. Wilcox, Fred A.: Investigation of a Continuous Normal-Shock Positioning Control on the Bypass of a Supersonic Inlet in Combination with the J34 Turbojet Engine. NACA RM E55J10, 1956.

3. Whalen, Paul P., and Wilcox, Fred A.: Use of Subsonic Diffuser Mach Number as a Supersonic-Inlet Control Parameter. NACA RM E56F05, 1956.

4. Wilcox, Fred, and Whalen, Paul: Dynamics of a Supersonic Inlet with Adjustable Bypass in Combination with a J34 Turbojet Engine. NACA RM E55L13a, 1956.

5. Beheim, Milton A., and Englert, Gerald W.: Effect of a J34 Turbojet Engine on Supersonic Diffuser Performance. NACA RM E55I21, 1956.

6. Keller, George R., and Buxton, Elliott R.: The Synthesis of Aircraft Hydraulic Servos. Preprint No. 839, SAE, 1956.

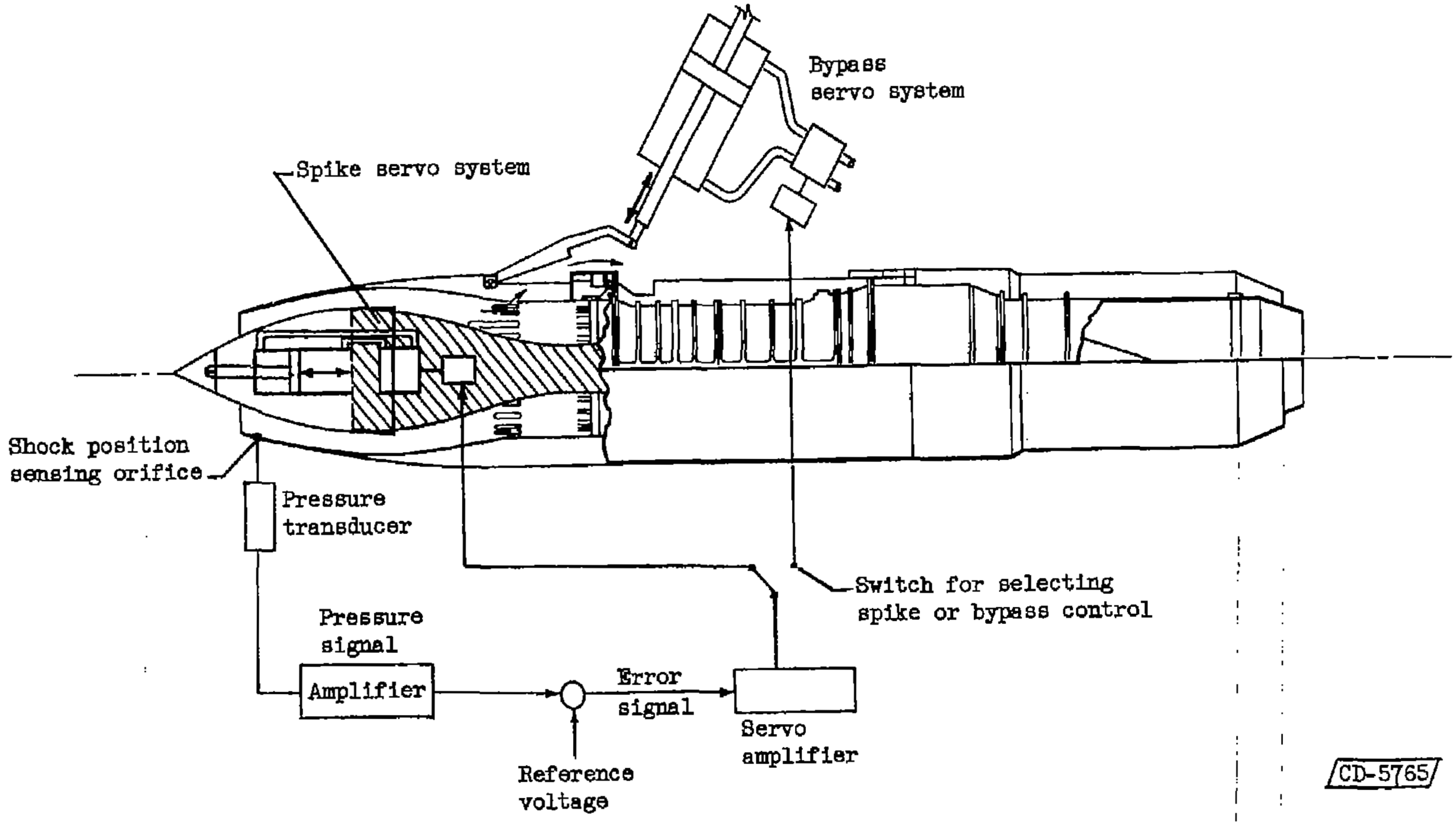

Figure 1. - Schematic diagram of control systems.

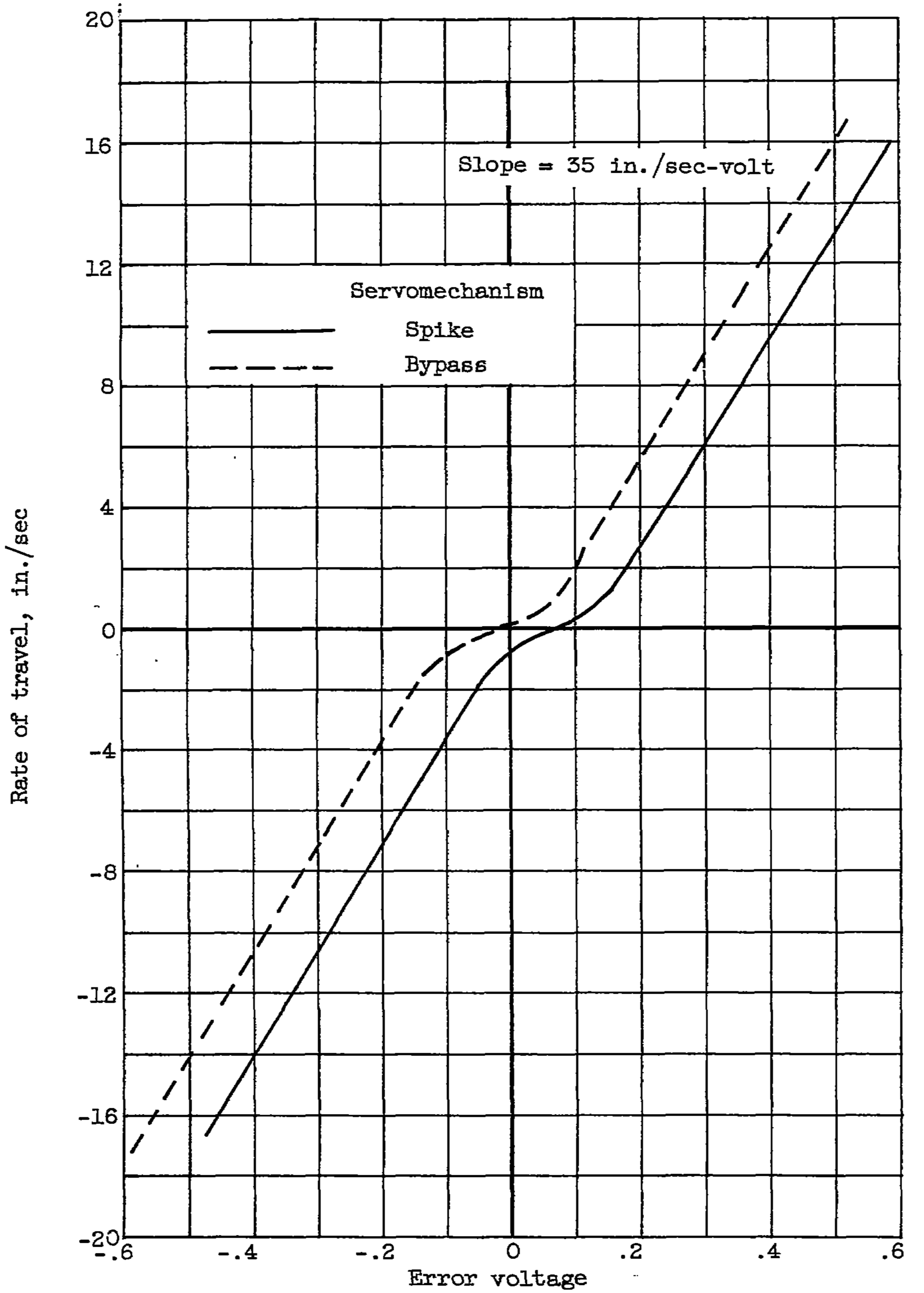

Figure 2. - Servomechanism gain.

4520

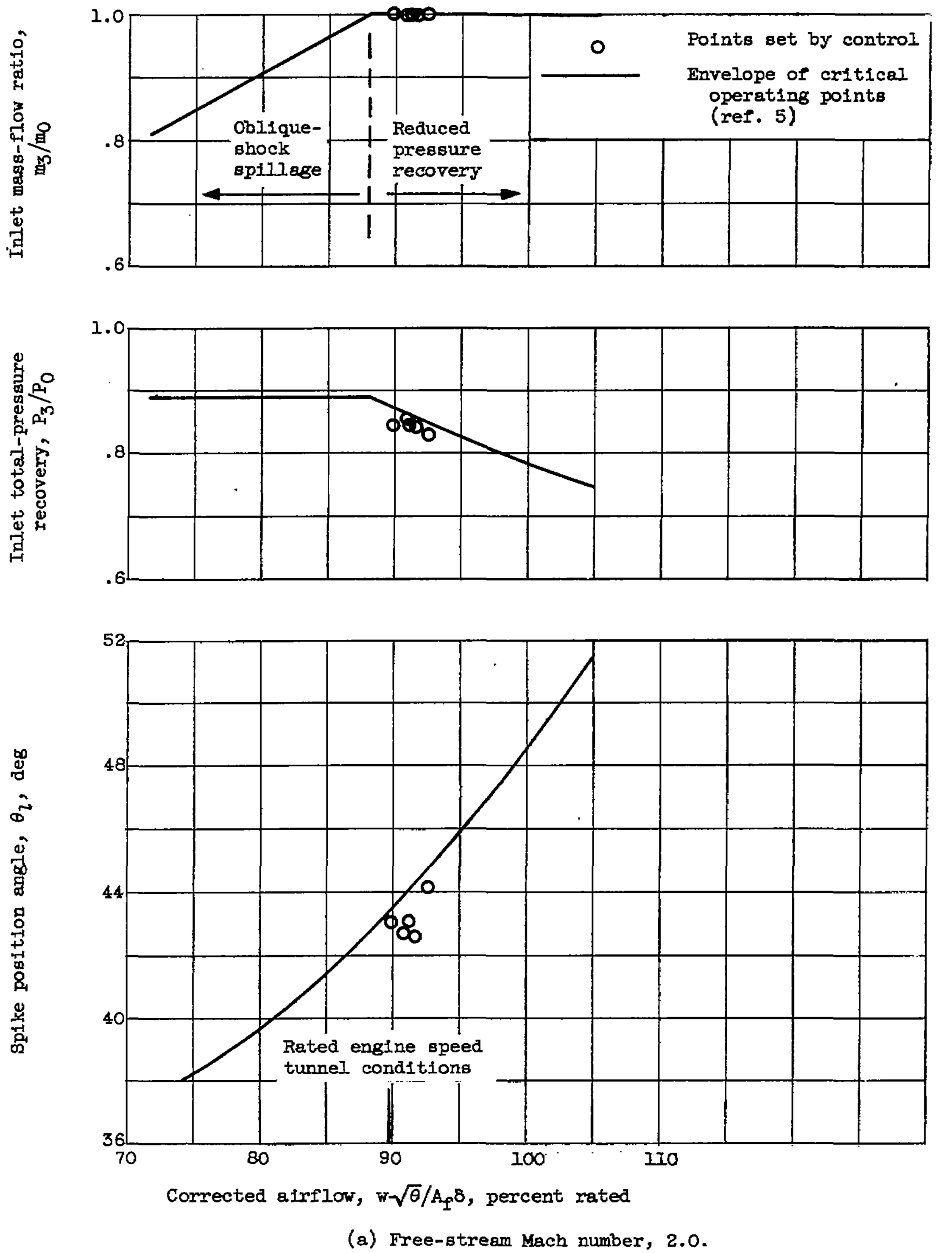

(a) Free-stream Mach number, 2.0.

Figure 3. - Operating points set by control.

4520

CH-2 back

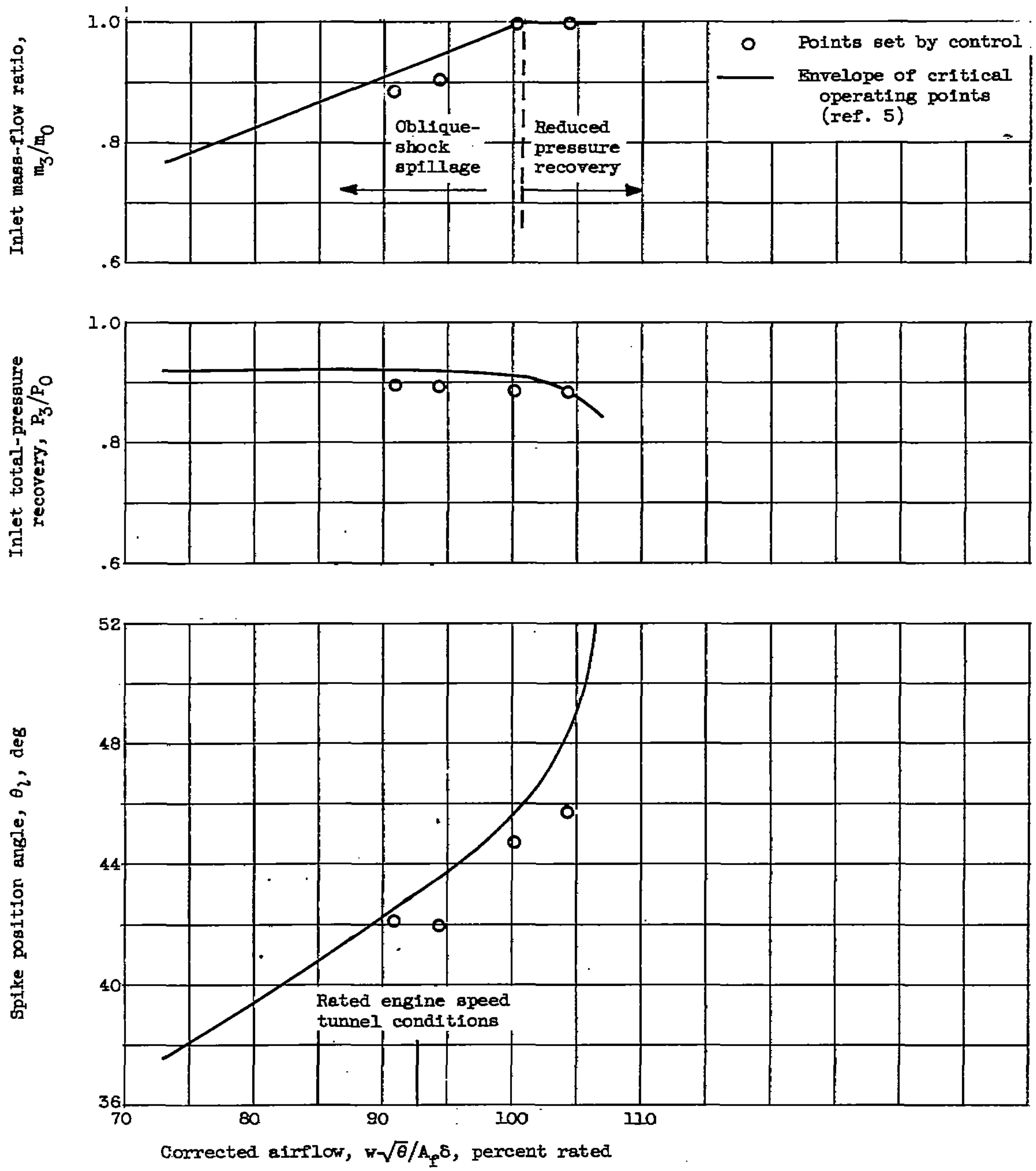

(b) Free-stream Mach number, 1.8.

Figure 3. - Concluded. Operating points set by control.

[redacted]

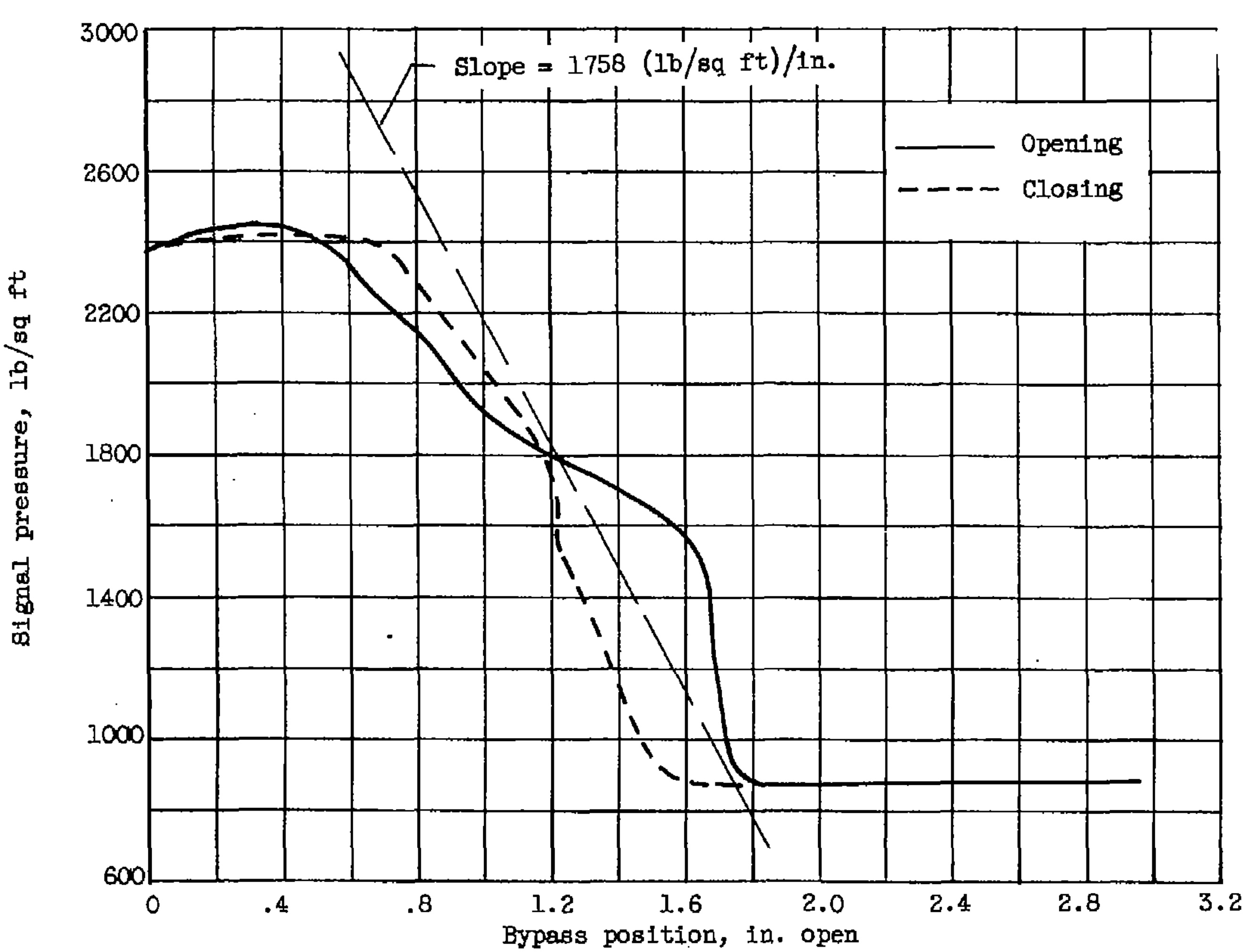

(a) Bypass control.

Figure 4. - Inlet gain in terms of servomotor linear position. Free-stream Mach number, 2.0.

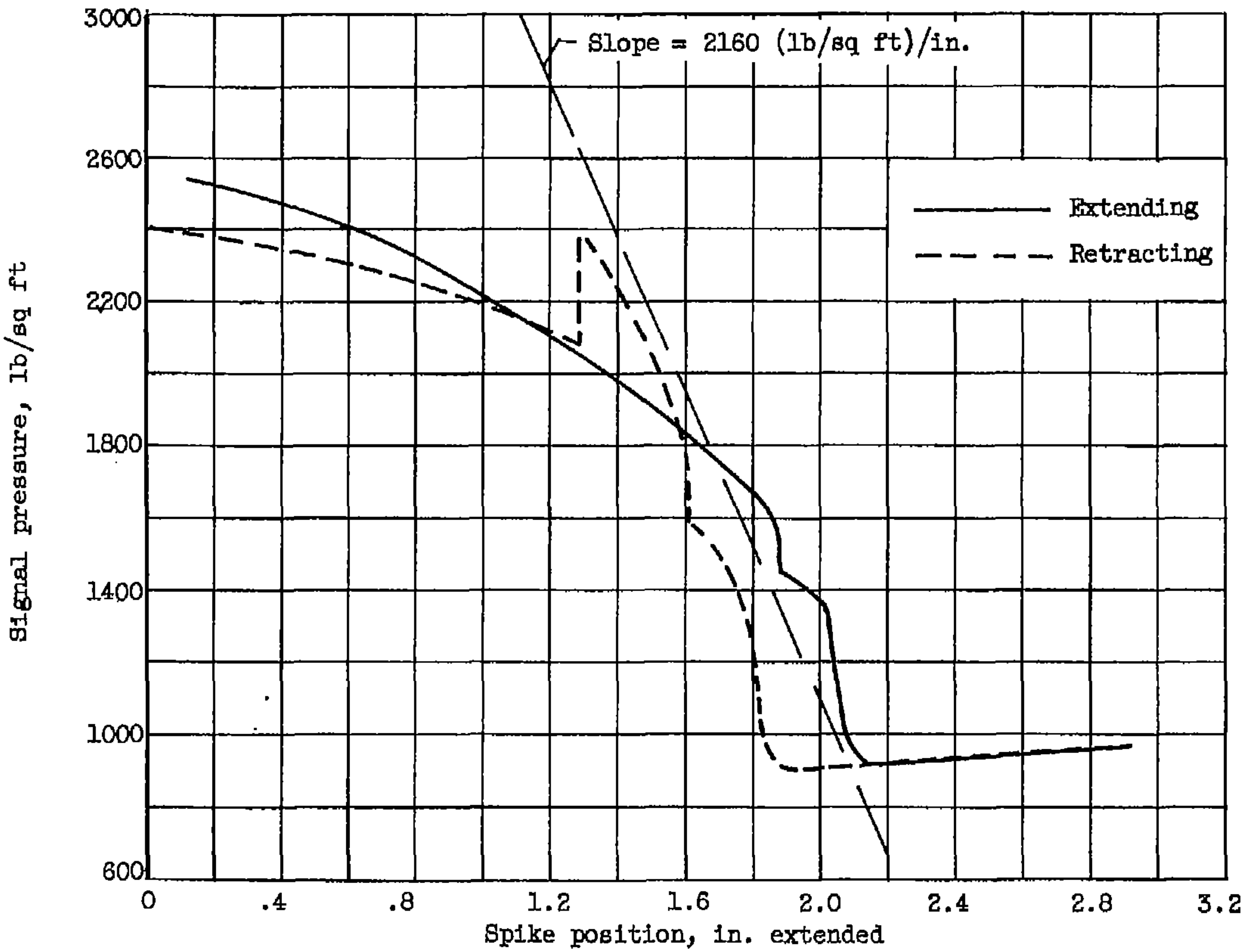

(b) Spike control.

Figure 4. - Concluded. Inlet gain in terms of servomotor linear position. Free-stream Mach number, 2.0.

4520

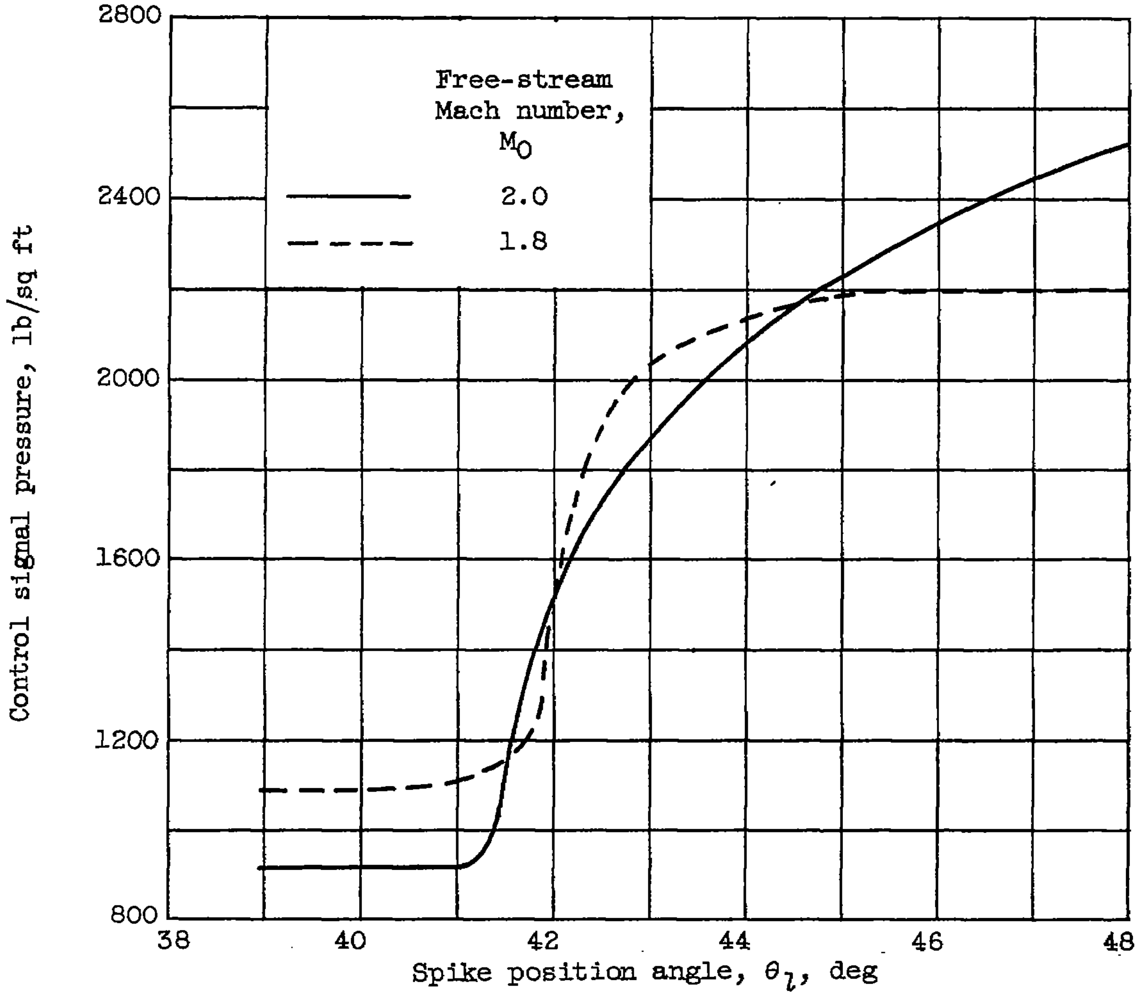

Figure 5. - Inlet gain in terms of spike position angle.

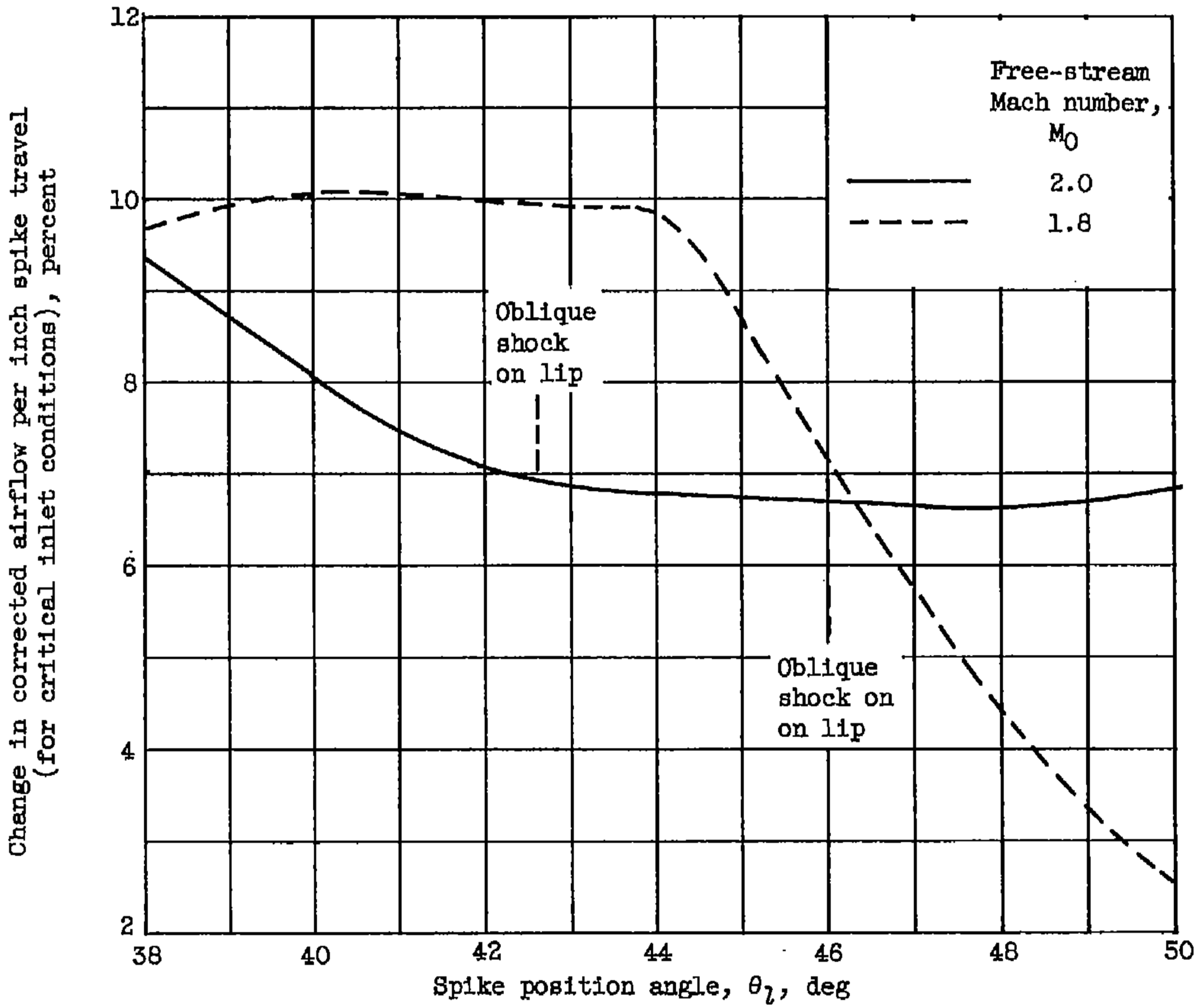

Figure 6. - Effectiveness of spike movement in controlling inlet corrected airflow for critical inlet conditions.

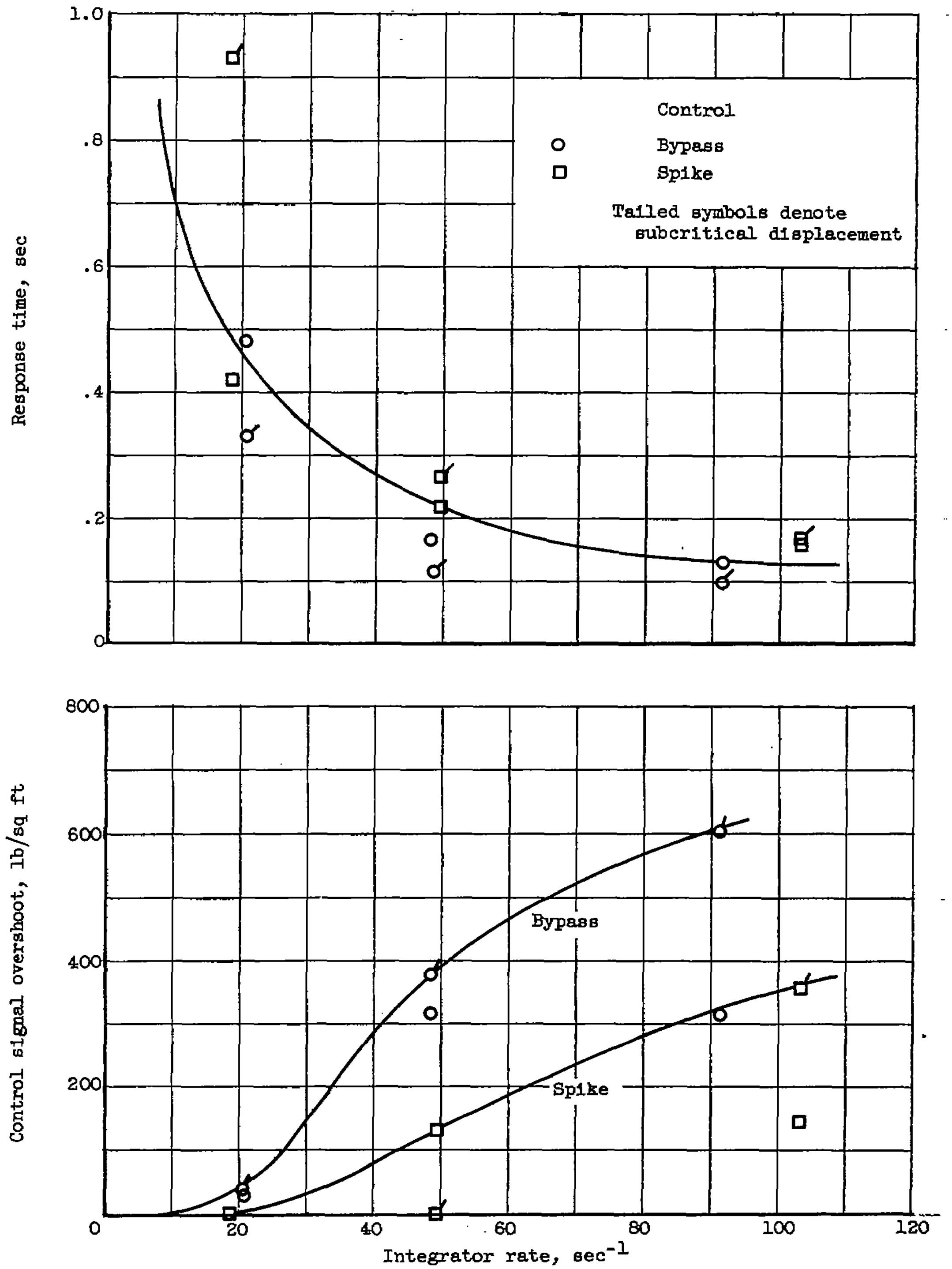

Figure 7. - Control response to manual disturbances of 10 percent of engine airflow. Free-stream Mach number, 2.0.

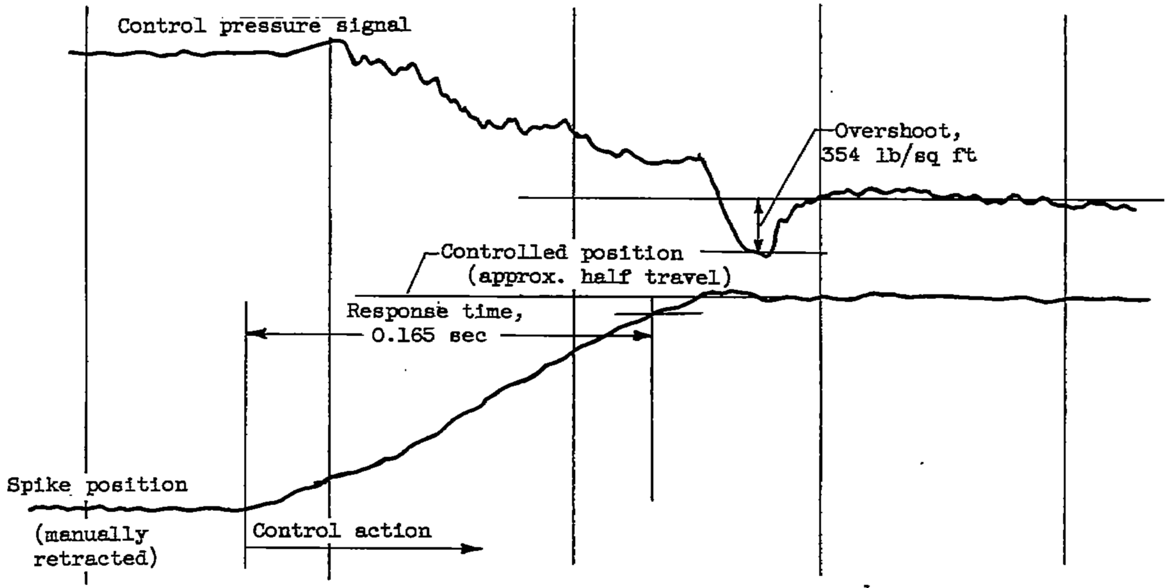

(a) Spike control; integrator rate, 103 seconds^{-1}.

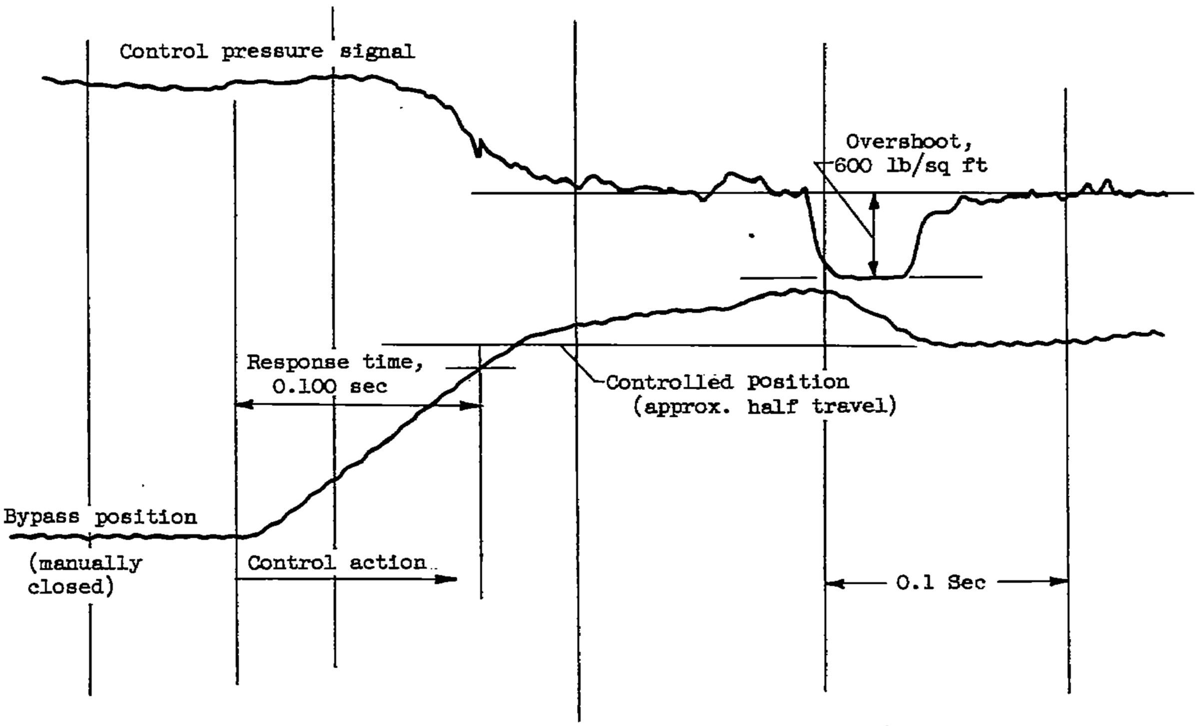

(b) Bypass control; integrator rate, 91.2 seconds^{-1}.

Figure 8. - Typical traces of control response. Free-stream Mach number, 2.0.

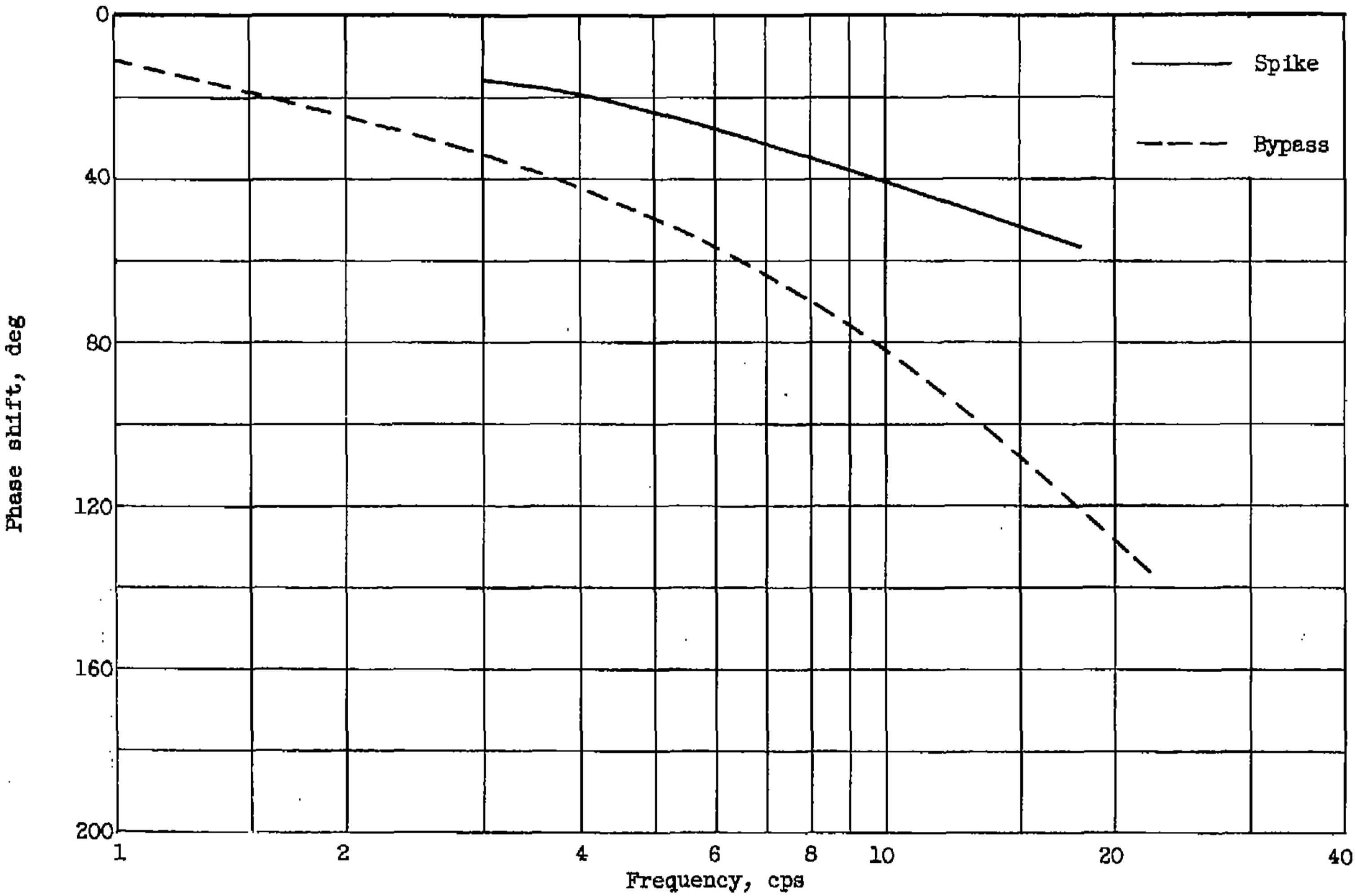

Figure 9. - Response of shock position sensing orifice to sinusoidal disturbances imposed by bypass and spike. Free-stream Mach numbers, 1.8 and 2.0.

[redacted]

NOTES: (1) Reynolds number is based on the diameter of a circle with the same area as that of the capture area of the inlet.

(2) The symbol * denotes the occurrence of buzz.

	Description			Test parameters				Test data				Performance		
eport and acility	Configuration	Number of oblique shocks	Type of boundary-layer control	Free-stream Mach number	Reynolds number $\times 10^{-6}$	Angle of attack, deg	Angle of yaw, deg	Drag	Inlet-flow profile	Discharge-flow profile	Flow picture	Maximum total-pressure recovery	Mass-flow ratio	Remarks
CONFID. M E57G16 ewis 8- y 6-foot uper- onic ind unnel	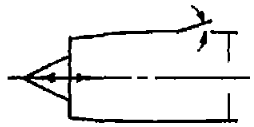	1	None	1.8 2.0	7.85 7.85	0 0	0 0	-- --	--- ---	---- ----	--- ---	88.2 85.2	1.00 1.00	Performance of translating-spike control of inlet in combination with J34 engine.
CONFID. M E57G16 ewis 8- y 6-foot uper- onic ind unnel	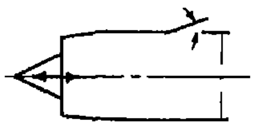	1	None	1.8 2.0	7.85 7.85	0 0	0 0	-- --	--- ---	---- ----	--- ---	88.2 85.2	1.00 1.00	Performance of translating-spike control of inlet in combination with J34 engine.
CONFID. M E57G16 ewis 8- y 6-foot uper- onic ind unnel	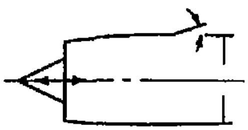	1	None	1.8 2.0	7.85 7.85	0 0	0 0	-- --	--- ----	---- ----	--- ---	88.2 85.2	1.00 1.00	Performance of translating-spike control of inlet in combination with J34 engine.
CONFID. M E57G16 ewis 8- y 6-foot uper- onic ind unnel	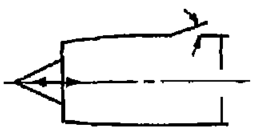	1	None	1.8 2.0	7.85 7.85	0 0	0 0	-- --	--- ---	---- ----	--- ---	88.2 85.2	1.00 1.00	Performance of translating-spike control of inlet in combination with J34 engine.

Bibliography

These strips are provided for the convenience of the reader and can be removed from this report to compile a bibliography of NACA inlet reports. This page is being added only to inlet reports and is on a trial basis.

[redacted]

[redacted]

[redacted]